Published in final edited form as:

Nano Lett. 2017 February 08; 17(2): 821–826. doi:10.1021/acs.nanolett.6b04071.

Improving T Cell Expansion with a Soft Touch

Lester H. Lambert[1,§], **Geraldine K.E. Goebrecht**[1,§], **Sarah E. De Leo**[1], **Roddy S. O'Connor**[2], **Selene Nunez-Cruz**[4], **Tai-De Li**[3], **Jinglun Yuan**[1], **Michael C. Milone**[2,4], and **Lance C. Kam**[1,*]

[1]Department of Biomedical Engineering, Columbia University, New York, NY 10027, USA

[2]Department of Pathology and Laboratory Medicine, Perelman School of Medicine at the University of Pennsylvania, Philadelphia, PA 19104, USA

[3]Advanced Science Research Center of CUNY, New York, NY 10031

[4]Center for Cellular Immunotherapies, Perelman School of Medicine at the University of Pennsylvania, Philadelphia, PA 19104, USA

Abstract

Protein-coated microbeads provide a consistent approach for activating and expanding populations of T cells for immunotherapy, but don't fully capture the properties of antigen presenting cells. In this report, we enhance T cell expansion by replacing the conventional, rigid bead with a mechanically soft elastomer. Polydimethylsiloxane (PDMS) was prepared in a microbead format and modified with activating antibodies to CD3 and CD28. Three different formulations of PDMS provided an extended proliferative phase in both $CD4^+$-only and mixed $CD4^+/CD8^+$ T cell preparations. $CD8^+$ T cells retained cytotoxic function, as measured by a set of biomarkers (perforin production, LAMP2 mobilization, and IFN-γ secretion) and an in vivo assay of targeted cell killing. Notably, PDMS beads presented a nanoscale polymer structure and higher rigidity than associated with conventional bulk material. These data suggest T cells respond to this higher rigidity, indicating an unexpected effect of curing conditions. Together, these studies demonstrate that adopting mechanobiology ideas into the bead platform can provide new tools for T cell-based immunotherapy.

Keywords

T cell; Mechanobiology; Immunotherapy; Nanoscale rigidity

A key step in emerging cellular immunotherapy approaches is ex vivo activation and expansion of T cells, which provides both a clinically effective number of cells and the opportunity to modify them through the introduction of genetic material or other

*Corresponding Author; lk2141@columbia.edu, ph: 1 (212) 854-8611.
§These authors contributed equally to this work

Supporting Information. Details on the experimental methods are included in the Supporting Information. This material is available free of charge via the Internet at http://pubs.acs.org

Author contributions

LL, GKEG, SED, RSO, SNC, TDL, and JY conducted experiments and acquired data. LL, GKEG, MCM, and LCK designed experiments, analyzed data, and prepared the manuscript.

manipulation. Early studies used autologous antigen presenting cells (APCs) for stimulation, but the desire for more consistent, reliable expansion spurred development of alternative platforms[1–6]. Microscale polystyrene beads, notably the Dynabeads system, provide a large stimulation area per culture volume and represent a successful example of such replacements. However, this synthetic system does not fully replicate the complex properties of APCs[7–8]. In this report, we improve the performance of the microbead platform by reducing the stiffness of the bead material, inspired by the softer mechanical properties of living cells. In a previous study, planar sheets of polydimethylsiloxane (PDMS) elastomer were modified with antibodies to CD3 and CD28 then used as an activating substrate[9]. Changing the concentration of crosslinker produced a series of substrates ranging in Young's modulus, E, from 5 MPa to 50 kPa. Intriguingly, populations of T cells stimulated on this substrate showed an extended proliferative phase and associated increase in cell production with decreasing rigidity. In this report, PDMS is prepared in a spherical form, leveraging the effect of substrate rigidity in the successful microbead format.

To transform the planar surfaces into a bead format capable of producing clinically relevant numbers of cells, we chose an emulsion-based approach, driven by the scalability of this method. PDMS pre-polymer (which is hydrophobic) was dispersed by agitation into small particles into an aqueous phase, using a surfactant to stabilize the individual droplets during a subsequent curing phase. Commonly available detergents, including Pluronic® and Triton™ X-100, provided good stabilization of the PDMS emulsion, but the inertness of their aqueous-facing groups hindered subsequent attachment of the activating antibodies needed to induce T cell activation. To facilitate this protein immobilization, human serum albumin (HSA) was used as the surfactant, as outlined in Figure 1A. The biosafety of recombinant HA is widely recognized, and this protein was previous used to immobilize biomolecules to preformed PDMS micro-channels[10].

The emulsion approach was applied to three different commercial formulations of PDMS, including the ubiquitous Sylgard 184, which when cured under conventional conditions produces materials with E of 2 MPa. We also examined MED-6215 and MED-4086 (NuSil), two medical-grade formulations which when prepared following the manufacturer guidelines present E of 500 and 50 kPa, respectively. This process was effective in producing beads from all three formulations, yielding spheres of diameter ranging from a few to tens of micrometers in size (Figure 1B). Notably, a large fraction of these beads presented diameters of 5 – 10 μm, similar to Dynabeads (4.5 μm). However, these preparations also included beads of smaller, few-micrometer size. These smaller beads pose a challenge in comparing PDMS beads and Dynabeads, as beads with diameter less than 3 μm are ineffective in activating T cells[11–12]. To remove these smaller structures, PDMS beads were sieved through a series of meshes, each presenting a defined opening size. Unfortunately, available meshes did not provide good selectivity of beads in the range of 5 μm. Also, the rate at which beads can be filtered decreases with opening size (since a smaller fraction of the mesh allows beads to pass through), making routine isolation of beads in the 5 – 10 micrometer range impractical for this study. As such, this report focuses predominantly on beads of 28 – 40 μm diameter, based on the throughput and performance of meshes with openings of these sizes. Examples of beads composed of Sylgard 184 are presented in Figures 1B&C, but these methods were effective in producing similar beads of all three PDMS formulations. It

is recognized that the curing conditions employed in this emulsion approach are quite different from those conventionally used for casting/shaping PDMS; in particular, the rigid surfaces normally used to define the shape and contours of the resultant PDMS are missing, raising the possibility that the surface topography of beads might not be well defined. The nanoscale topography of beads, prepared to this cured, HA-presenting stage, was thus examined by atomic force microscopy (AFM). As illustrated in Figure 1D, these surfaces presented irregular hills, measuring tens of nanometers in both extent on the bead surface and height. While the overall topography was similar between PDMS formulations, a small effect on surface roughness was observed. Beads composed of Sylgard 184, MED-6215, and MED-4086 presented root mean square surface roughness, Rq, factors of 15.2 ± 6.9, 14.6 ± 8.1, and 4.3 ± 0.8 nm (mean ± s.d, n = 5 beads for each composition), respectively; Rq of Sylgard 184 was significantly greater than that of MED-4086, with no difference detected for all other comparisons (α=0.05). Previous reports demonstrated the ability of T cells to recognize nanoscale topographies[13–14], but on the order of hundreds of nanometers; the dimensions detected here are much smaller, closer to the scale of individual proteins. It is unlikely that the surface roughness detected here influences T cell response.

This approach was highly scalable: 10 mL of PDMS produced typically 1×10^7 beads within the 28 – 40 μm diameter range. This method is also versatile; in Figure 1E, magnetite nanoparticles were incorporated into the PDMS before curing, producing beads that can be collected from solution using a magnetic field.

For expansion of T cells, PDMS beads were modified with activating antibodies to CD3 and CD28 (clones OKT3 and 9.3) using an intermediary layer of Protein A that was covalently attached to the albumin (Figures 1A&C). The amount of protein attached to the beads was measured semi-quantitatively using flow cytometry to asses fluorescently-labeled OKT3 (A488-OKT3), comparing this signal against a set of calibration standards (Figure S1). This method, together with adjustment of Protein A concentration, was used to ensure a consistent level of protein attachment across polymer formulations and preparation batches (Figure S1). In addition, a standard level of antibody attachment (as measured by flow cytometry of A488-OKT3) that provides consistent activation of cells was established in an initial set of experiments.

The ability of PDMS beads to expand cells was first examined with primary human $CD4^+/CD8^+$ T cells. Cells were combined with beads at a 1 : 3 ratio (cells : beads), then cultured under standard culture conditions. Cells initially attached to the beads (Figure S2), but by 2 days of culture, largely released from the surface and entered expansion, similar to that observed for planar PDMS[9]. On day three, cells were re-plated into new wells, increasing the culture volume with fresh media to maintain a concentration of 1×10^6 cells/mL; this dilution of the cell culture volume was then carried out every second day after day 3. While not actively collected and separated from the cells, the beads, being denser than cells, were largely removed from growing cells at day three. In a typical expansion, cells undergo several days of rapid proliferation followed by a decrease in cell division as the population comes to rest (Figure 2A). The phase of rapid cell division lasts about 1 week for cells stimulated using the Dynabeads platform. By comparison, cells activated with any of the PDMS formulations produced a longer proliferative phase and consequently greater

yield of cells in each process, illustrated in the representative expansion of Figure 2A. Figure 2B compares the maximum cell population (reported as population doublings), used here as a measure of expansion efficiency, from a single donor and across several donors, demonstrating that the three PDMS formulations provide greater cell production than Dynabeads. Variability between different runs from a single donor was similar to that across donors. Figure 2C compares the percentage of cells that entered division and proliferative index as a function of stimulation system, measured at Day 3 of culture. No major effect of bead material was observed, indicating that the enhanced expansion observed on PDMS is not simply due to higher efficiency in activation. In addition, cells activated with PDMS beads show a different profile of cell volume than those treated with Dynabeads, decreasing back towards a resting volume (Figure 2D) on a longer timescale, consistent with an extended proliferative phase. For the functional assays presented in the following sections, cells from each expansion were collected and frozen when average size dropped below 400 fL.

Surprisingly, no difference was detected between PDMS formulations with regards to cell expansion (Figure 2A,B). It is noted that Dynabeads are smaller (4.5 μm diameter) than the PDMS beads. To address the possibility that enhanced performance of the PDMS structures was related to bead diameter, cell expansion was compared between PDMS beads and polystyrene beads of 25 μm diameter, coated with the same sequence of proteins (Figure 2E). Replicating the antibody immobilization strategy developed for PDMS but on the polystyrene beads allowed a better examination of the effect of rigidity, as the orientation, concentration, and even identity of activating antibodies on Dynabeads, while optimized, are proprietary; it is not possible to ensure that the details of antibody presentation on Dynabeads are fully captured on the PDMS beads. Flow cytometry of beads presenting A488-OKT3 was again used to assure that similar amounts of antibodies were immobilized onto the polystyrene and PDMS beads (Figure S1). Comparisons of T cell expansion across these beads were carried out with primary human $CD4^+$ T cells. Expansion with PDMS beads produced more population doublings than Dynabeads (Figure 2E), showing the same increase in proliferation phase and population doublings as mixed $CD4^+/CD8^+$ cells (Figure 2A&B). Expansion of cells using rigid polystyrene beads was similar to that obtained with Dynabeads, indicating that the larger size of the PDMS beads does not fully explain enhanced expansion seen on those materials. Finally, the effect of bead size was tested using MED-4086 PDMS beads that were sieved into size ranges of 20 – 30 μm and 6 – 10 μm. As shown in Figure S2B&C, expansion of mixed $CD4^+/CD8^+$ T cells was independent of bead size, and enhanced across all MED-4086 beads compared to Dynabeads. Together, these experiments indicate that bead dimension has at most a modest effect on cell expansion.

While PDMS beads provided more doublings of T cells than Dynabeads in a single expansion, the benefit of obtaining more cells would be minimal if they are not functional. In this direction, three measures of $CD8^+$ T cell function – production of perforin, mobilization of LAMP2, and secretion of IFN-γ – were compared across the different platforms. Mixed $CD4^+/CD8^+$ T cells were activated using the PDMS platforms, and then restimulated at the end of expansion and assayed for these functions. The data in Figure 3A focuses on $CD8^+$ T cells from these mixed populations. As showed in that figure, cells

expanded on PDMS beads were functional and not dramatically different from those activated with Dynabeads.

Functionality of T cells expanded using PDMS beads was also examined in a mouse xenograft model. Nalm-6 cells, a human B cell precursor cell line, were injected into NSG mice and allowed to engraft, establishing a model of acute lymphoblastic leukemia (ALL). The Nalm-6 cells contained a luciferase gene, allowing measurement of ALL load by bioluminescent imaging; by day 7, total flux of bioluminescence intensity was on the order of 1×10^7 within individual animals. Six days after Nalm-6 introduction, primary human $CD4^+/CD8^+$ T cells modified with a chimeric antigen receptor (CAR) to CD19 (CD19BBz, prepared as previously described[15]) were injected into mouse tail-vein. Figure 3B compares Nalm-6 load up to 15 days after initial injection as a function of T cell preparation method. Injection of CD19BBz cells expanded with either MED-4086 beads or Dynabeads showed decreased Nalm-6 burden compared to their counterparts which were not transduced ($P < 0.001$). Furthermore, Nalm-6 luminescence in animals treated with CD19BBz cells expanded using MED-4086 beads was similar to that of animals for which Dynabeads were used; in vivo functionality of PDMS-expanded T cells is similar to those produced using Dynabeads.

While differences were observed between the PDMS and rigid polystyrene beads, the similar performance across PDMS formulations was unexpected, as these three materials in their conventional preparations exhibit Young's moduli covering almost two orders of magnitude. By manual manipulation, the rigidity of large (5 mm diameter) Sylgard 184, MED-6215, and MED-4086 beads resemble that of the bulk, conventionally-prepared material. However, it is possible that the emulsion format results in material surface properties that are different than those obtained under conventional curing; normally, PDMS is cured in contact with air or impermeable casting surface, producing a surface rigidity that is similar to bulk. To test this, the local, surface rigidity of PDMS beads was measured by atomic force microscopy (AFM); 8 nm radius tips were used, applying forces on the order of tens of nanoNewtons and resulting in deformations of tens of nanometers. Beads of 1 – 3 millimeter diameter were used for these measurements, given the limited lateral precision of the AFM in selecting a specific area of a sample. By this method, Sylgard 184 beads presented a rigidity of 7.3 MPa, 2 – 3 times higher than that associated with the conventional preparation (Figure 4A). The rigidities of MED-6215 and MED-4086 preparations were not significantly different from Sylgard 184, thus much higher than that of their conventional preparations. These values of Young's modulus are slightly higher than that explored in our earlier demonstrations of mechanosensing on PDMS[9], but two orders of magnitude lower than polystyrene (GPa) suggesting that T cell sensitivity to material rigidity extends into this higher range, albeit with lower responsiveness. These values of elastic modulus are much higher than the kilo-Pascal range normally associated with tissues[16], including lymph nodes[17]. However, those studies focus predominantly on integrin interactions with extracellular matrix proteins. The TCR/CD3 and CD28 receptors explored here have very different molecular contexts than integrins, most prominently weaker coupling with the underlying cytoskelelton[18–19]. Considering the TCR/CD3 complex as a molecular clutch engaging the actin cytoskeleton and extracellular environment, these more fugitive

interactions can explain a shift of mechanosensing sensitivity to these higher ranges of rigidity[20].

To understand the source of increased rigidity in the emulsion format, large (millimeter-scale) PDMS beads were sections and analyzed as a function of depth by AFM. Figure 4B illustrates a section of a MED-6215 bead, taken near the bead edge and covering 20 μm. Measurements of both topography and local modulus indicate a network of rigid regions, interspersed within a softer background; these features are absent in a corresponding section of MED-6215 cured under conventional conditions (Figure S3). These local domains may contribute to the higher rigidity observed on the bead preparations; overlaying local rigidity with the topography of the surface of a bead (Figure 4C) reveals a correlation between raised areas and modulus suggesting the presence of domains on at this interface that is presented to cells. These domains are found hundreds of micrometers into the emulsion-cured PDMS structure, so even the largest beads used for expansion in this report (28 – 40 μm) are potentially composed entirely of this hetereogenous nanostructure. It is also noted that the background, softer regions are still stiffer than the conventional counterpart; in the example of MED-6215 (Figure 4B) these intervening regions present a measured modulus on the order of 3 MPa. Together, the locally stiff domains and overall higher rigidity indicate that PDMS curing conditions can have large influences on material properties. Future studies to identify and then address these effects may produce beads with even greater enhancement of cell expansion. In summary, the approach of replacing rigid polystyrene beads with a softer elastomer has promise in making immunotherapy more effective and accessible to a wider range of patients.

Supplementary Material

Refer to Web version on PubMed Central for supplementary material.

Acknowledgments

This work was supported in part by the National Institutes of Health (PN2 EY016586 to LCK and MCM, R01 AI110593 to LCK), the National Science Foundation (through a GRFP to SED), and the Columbia-Coulter Translational Research Partnership.

References

1. Ratta M, Fagnoni F, Curti A, Vescovini R, Sansoni P, Oliviero B, Fogli M, Ferri E, Della Cuna GR, Tura S, Baccarani M, Lemoli RM. Dendritic cells are functionally defective in multiple myeloma: the role of interleukin-6. Blood. 2002; 100:230–237. [PubMed: 12070032]
2. Ruffini PA, Kwak LW. Immunotherapy of multiple myeloma. Semin Hematol. 2001; 38:260–267. [PubMed: 11486314]
3. Zheng CY, Ostad M, Andersson M, Celsing F, Holm G, Sundblad A. Natural cytotoxicity to autologous antigen-pulsed dendritic cells in multiple myeloma. Br J Haematol. 2002; 118:778–785. [PubMed: 12181045]
4. Della Bella S, Gennaro M, Vaccari M, Ferraris C, Nicola S, Riva A, Clerici M, Greco M, Villa ML. Altered maturation of peripheral blood dendritic cells in patients with breast cancer. Br J Cancer. 2003; 89:1463–1472. [PubMed: 14562018]
5. Oelke M, Krueger C, Schneck JP. Technological advances in adoptive immunotherapy. Drugs Today. 2005; 41:13–21.

6. Andres PG, Howland KC, Dresnek D, Edmondson S, Abbas AK, Krummel MF. CD28 Signals in the Immature Immunological Synapse. J Immunol. 2004; 172:5880–5886. [PubMed: 15128767]
7. Turtle CJ, Delrow J, Joslyn RC, Swanson HM, Basom R, Tabellini L, Delaney C, Heimfeld S, Hansen JA, Riddell SR. Innate signals overcome acquired TCR signaling pathway regulation and govern the fate of human CD161(hi) CD8alpha(+) semi-invariant T cells. Blood. 2011; 118:2752–62. [PubMed: 21791427]
8. Eggermont LJ, Paulis LE, Tel J, Figdor CG. Towards efficient cancer immunotherapy: advances in developing artificial antigen-presenting cells. Trends Biotechnol. 2014; 32:456–65. [PubMed: 24998519]
9. O'Connor RS, Hao X, Shen K, Bashour K, Akimova T, Hancock WW, Kam LC, Milone MC. Substrate Rigidity Regulates Human T Cell Activation and Proliferation. J Immunol. 2012; 189:1330–9. [PubMed: 22732590]
10. Eteshola E, Leckband D. Development and characterization of an ELISA assay in PDMS microfluidic channels. Sens Actuators, B. 2001; 72:129–133.
11. Mescher MF. Surface contact requirements for activation of cytotoxic T lymphocytes. J Immunol. 1992; 149:2402–5. [PubMed: 1527386]
12. Wei X, Tromberg BJ, Cahalan MD. Mapping the sensitivity of T cells with an optical trap: polarity and minimal number of receptors for Ca(2+) signaling. Proc Natl Acad Sci U S A. 1999; 96:8471–6. [PubMed: 10411899]
13. Hu J, Gondarenko AA, Dang AP, Bashour KT, O'Connor RS, Lee S, Liapis A, Ghassemi S, Milone MC, Sheetz MP, Dustin ML, Kam LC, Hone JC. High-Throughput Mechanobiology Screening Platform Using Micro- and Nanotopography. Nano Lett. 2016; 16:2198–204. [PubMed: 26990380]
14. Kwon KW, Park H, Doh J. Migration of T cells on surfaces containing complex nanotopography. PLoS One. 2013; 8:e73960. [PubMed: 24069255]
15. Milone MC, Fish JD, Carpenito C, Carroll RG, Binder GK, Teachey D, Samanta M, Lakhal M, Gloss B, Danet-Desnoyers G, Campana D, Riley JL, Grupp SA, June CH. Chimeric receptors containing CD137 signal transduction domains mediate enhanced survival of T cells and increased antileukemic efficacy in vivo. Mol Ther. 2009; 17:1453–64. [PubMed: 19384291]
16. Levental I, Georges PC, Janmey PA. Soft biological materials and their impact on cell function. Soft Matter. 2007; 3:299–306.
17. Miyaji K, Furuse A, Nakajima J, Kohno T, Ohtsuka T, Yagyu K, Oka T, Omata S. The stiffness of lymph nodes containing lung carcinoma metastases: a new diagnostic parameter measured by a tactile sensor. Cancer. 1997; 80:1920–5. [PubMed: 9366294]
18. Smoligovets AA, Smith AW, Wu HJ, Petit RS, Groves JT. Characterization of dynamic actin associations with T-cell receptor microclusters in primary T cells. J Cell Sci. 2012; 125:735–42. [PubMed: 22389407]
19. Yu, C-h, Wu, H-J., Kaizuka, Y., Vale, RD., Groves, JT. Altered Actin Centripetal Retrograde Flow in Physically Restricted Immunological Synapses. PLoS ONE. 2010; 5:e11878. [PubMed: 20686692]
20. Bangasser BL, Rosenfeld SS, Odde DJ. Determinants of maximal force transmission in a motor-clutch model of cell traction in a compliant microenvironment. Biophys J. 2013; 105:581–92. [PubMed: 23931306]
21. Semnani RT, Keiser PB, Coulibaly YI, Keita F, Diallo AA, Traore D, Diallo DA, Doumbo OK, Traore SF, Kubofcik J, Klion AD, Nutman TB. Filaria-induced monocyte dysfunction and its reversal following treatment. Infect Immun. 2006; 74:4409–17. [PubMed: 16861626]

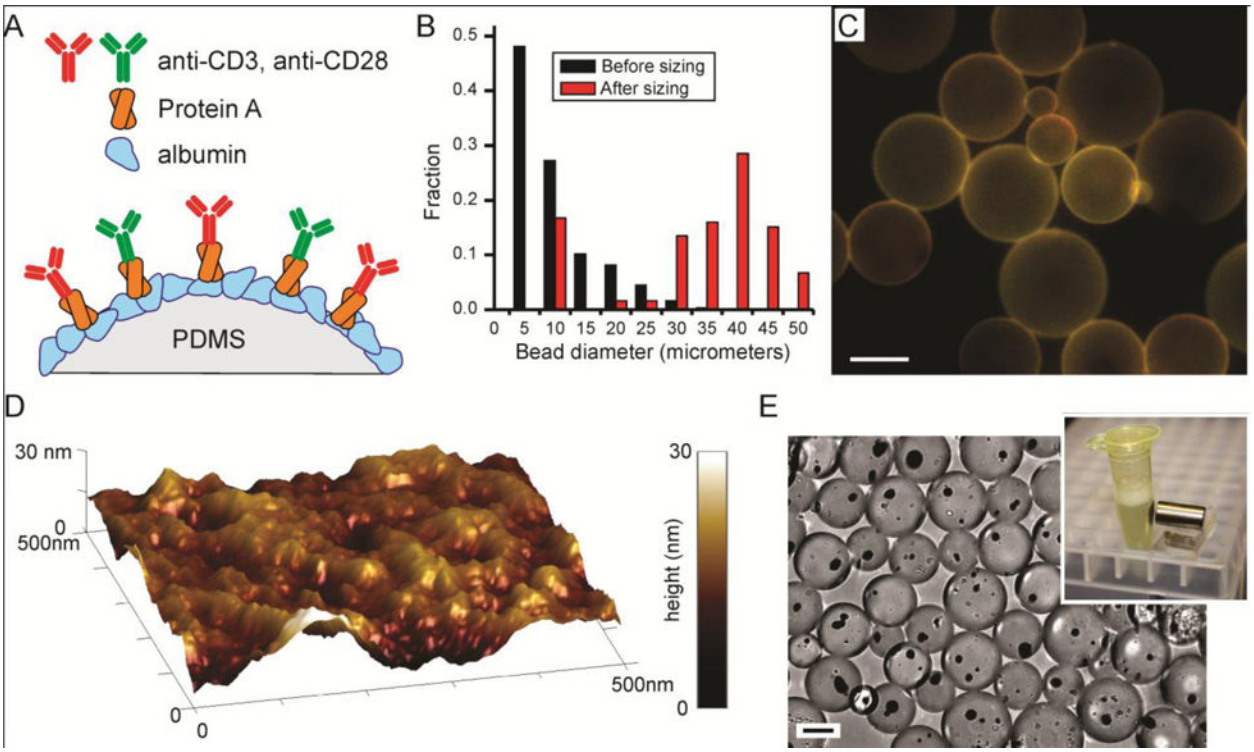

Figure 1. Scalable production of PDMS beads

(**A**) Molecular strategy for attaching anti-CD3 and anti-CD28 to PDMS beads. (**B**) Sieving isolates beads within a desired range of diameters. Data from a representative preparation of Sylgard 184 beads. (**C**) Sylgard 184 beads, illustrating morphology and size distribution. PDMS was stained with Nile Red (red), while OKT3 (green, anti-CD3) was labeled with Alexa 488. Scale bar = 25 μm. (**D**) Topography of a representative PDMS bead composed of Sylgard 184. This image shows a 500 nm × 500 nm patch, with vertical topography represented by surface color (corresponding to range bar). (**E**) Incorporation of magnetic particles into PDMS beads allow collection.

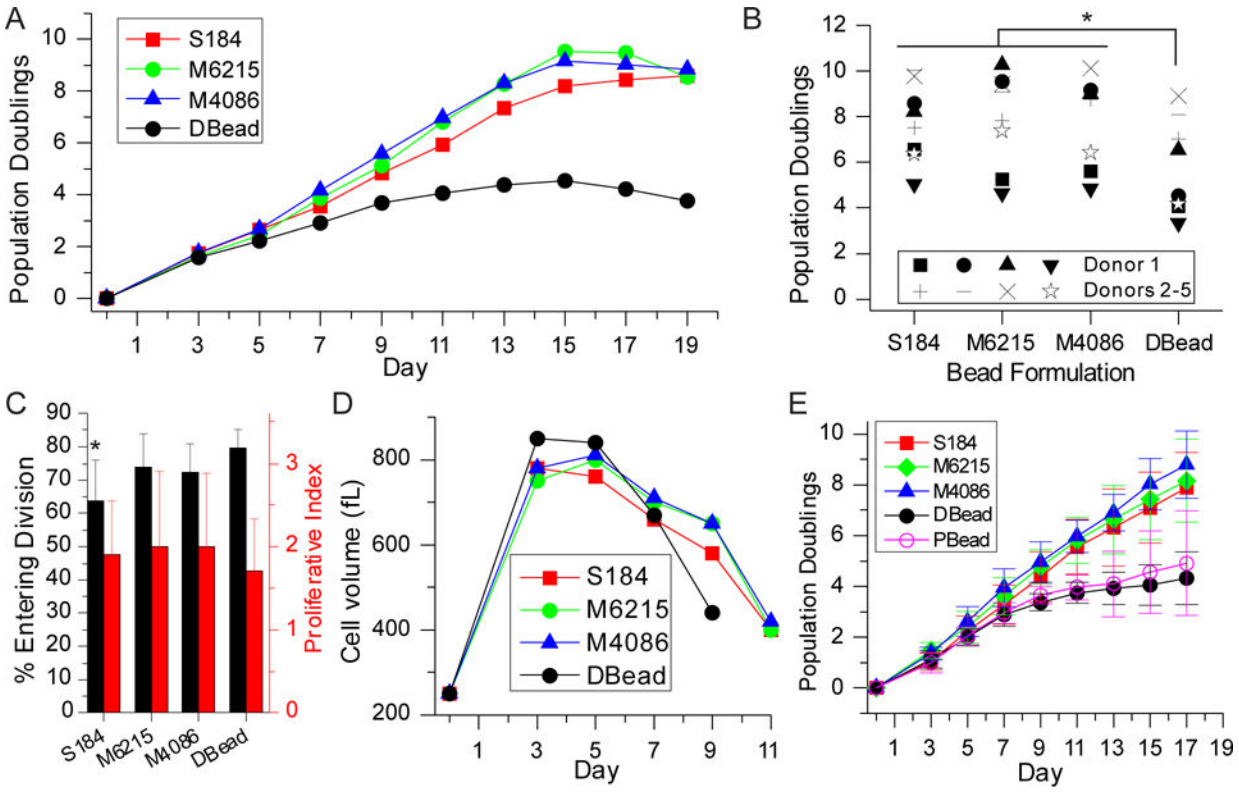

Figure 2. PDMS beads provide extended proliferation

(**A**) Expansion of mixed $CD4^+/CD8^+$ T cells using PDMS beads provided additional divisions compared to Dynabeads. (**B**) Comparison of maximum doublings reached using PDMS beads vs. Dynabeads. * $P < 0.0001$. (**C**) Three-day expansion of $CD4^+/CD8^+$ T cells. * $P < 0.05$. (**D**) Cells expanded using PDMS beads returned to a resting volume later than those activated using Dynabeads. (**E**) Comparison of $CD4^+$ T cell expansion using PDMS beads, Dynabeads, and rigid polystyrene. Data are mean ± s.d., n = 4. At Day 17, DBead is different from S184, M6215, and M4086, $P < 0.05$. In addition, PBead is different from M6215 and M4086, $P < 0.05$. S184 = Sylgard 184, M6215 = MED-6215, M4086 = MED-4086, DBead = Dynabeads, and PBead = 25 μm-diameter polystyrene beads. All statistical analyses were conducted using 2-way ANOVA and Tukey's HSD methods.

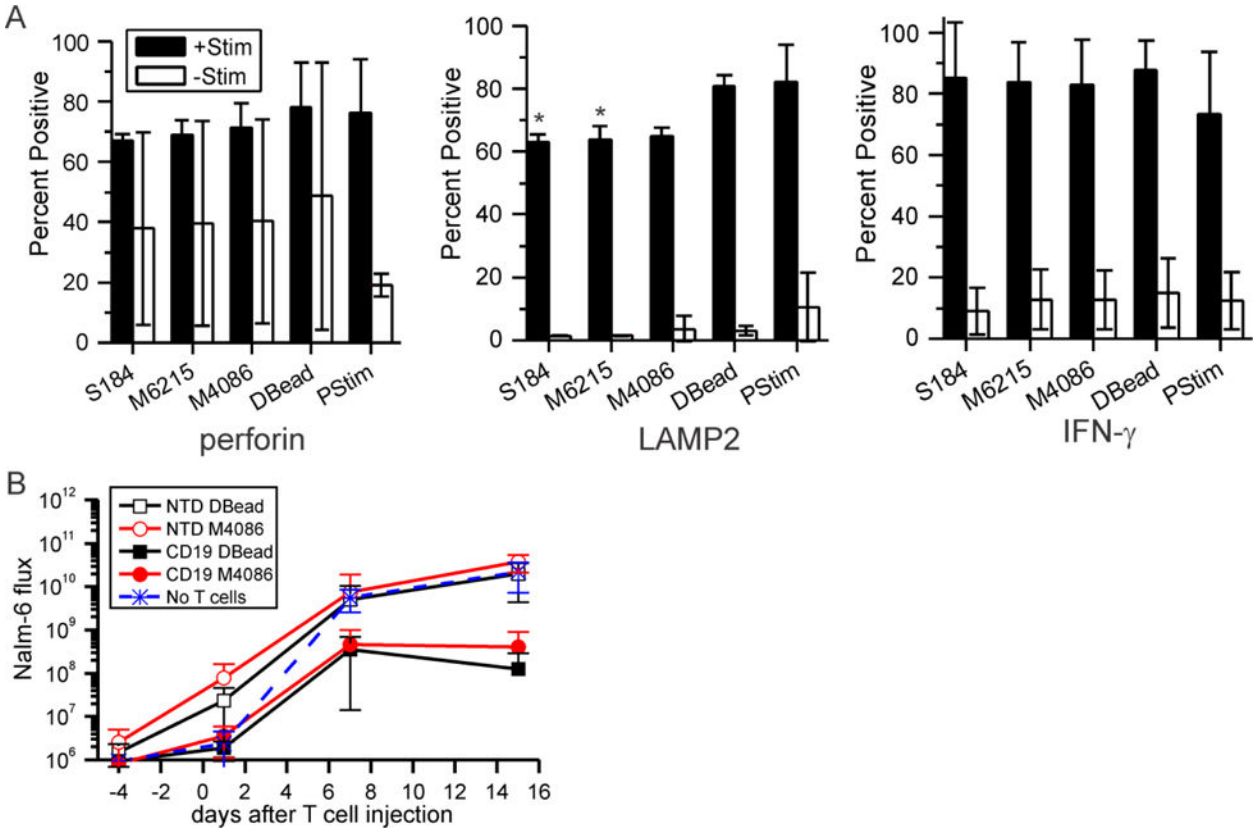

Figure 3. Mixed CD4$^+$/CD8$^+$ T cells expanded on PDMS are functional

(**A**) T cells were expanded on each platform, restimulated with Dynabeads (+Stim), and then assayed for three measured of functionality. Control cells (-Stim) were not activated with anti-CD3/anti-CD28 beads. Data are mean ± s.d., n = 3; * $P < 0.05$ compared to Dynabeads control. S184 = Sylgard 184, M6215 = MED-6215, M4086 = MED-4086, DBead = Dynabeads, and PStim = initial activation. Statistical analyses were conducted using 2-way ANOVA and Tukey's HSD methods. (**B**) Injection of CD19BBz CAR T cells into mice reduced load of Nalm-6 cells, a model of ALL, compared to their non-transduced counterparts (NTS). The average of ventral and dorsal readings was measured for each mouse at each time point (days after injection of T cells) Data are mean ± s.d., n = 5 – 8 mice per group. Lower whiskers, indicating mean – s.d, are omitted if not presentable on the log axis. Statistical analyses were conducted at each time point using 1-way ANOVA and Tukey's HSD methods; see main text for comparisons.

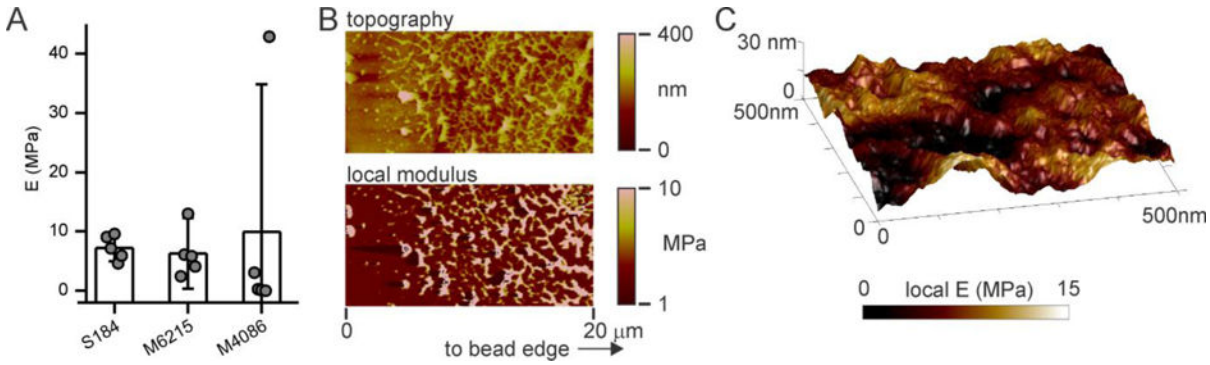

Figure 4. PDMS beads present high surface stiffness and nanoscale structure

(**A**) Comparison of Young's modulus across PDMS beads of different formulations. Each data point represents the average modulus measured for an individual bead, with five beads measured for each condition. Data bars represent mean ± s.d. across these beads. The modulus of an individual bead was calculated from five independent, 500 nm × 500 nm fields measured on that structure. (**B**) AFM analysis of a PDMS bead as a function of depth from the surface, sectioned from a large (millimeter-scale) MED-6215 bead. This representative region was within 500 μm of the bead edge. (**C**) Local rigidity analysis of the bead surface presented in Figure 1D, overlaying modulus (color coded, as indicated by the underlying bar) onto surface topography.